Global Polarization of Ξ and Ω Hyperons in Au + Au Collisions at $\sqrt{s_{NN}} = 200$ GeV

J. Adam,[6] L. Adamczyk,[2] J. R. Adams,[39] J. K. Adkins,[30] G. Agakishiev,[28] M. M. Aggarwal,[41] Z. Ahammed,[61] I. Alekseev,[3,35] D. M. Anderson,[55] A. Aparin,[28] E. C. Aschenauer,[6] M. U. Ashraf,[11] F. G. Atetalla,[29] A. Attri,[41] G. S. Averichev,[28] V. Bairathi,[53] K. Barish,[10] A. Behera,[52] R. Bellwied,[20] A. Bhasin,[27] J. Bielcik,[14] J. Bielcikova,[38] L. C. Bland,[6] I. G. Bordyuzhin,[3] J. D. Brandenburg,[6] A. V. Brandin,[35] J. Butterworth,[45] H. Caines,[64] M. Calderón de la Barca Sánchez,[8] D. Cebra,[8] I. Chakaberia,[29,6] P. Chaloupka,[14] B. K. Chan,[9] F-H. Chang,[37] Z. Chang,[6] N. Chankova-Bunzarova,[28] A. Chatterjee,[11] D. Chen,[10] J. Chen,[49] J. H. Chen,[18] X. Chen,[48] Z. Chen,[49] J. Cheng,[57] M. Cherney,[13] M. Chevalier,[10] S. Choudhury,[18] W. Christie,[6] X. Chu,[6] H. J. Crawford,[7] M. Csanád,[16] M. Daugherity,[1] T. G. Dedovich,[28] I. M. Deppner,[19] A. A. Derevschikov,[43] L. Didenko,[6] X. Dong,[31] J. L. Drachenberg,[1] J. C. Dunlop,[6] T. Edmonds,[44] N. Elsey,[63] J. Engelage,[7] G. Eppley,[45] S. Esumi,[58] O. Evdokimov,[12] A. Ewigleben,[32] O. Eyser,[6] R. Fatemi,[30] S. Fazio,[6] P. Federic,[38] J. Fedorisin,[28] C. J. Feng,[37] Y. Feng,[44] P. Filip,[28] E. Finch,[51] Y. Fisyak,[6] A. Francisco,[64] L. Fulek,[2] C. A. Gagliardi,[55] T. Galatyuk,[15] F. Geurts,[45] N. Ghimire,[54] A. Gibson,[60] K. Gopal,[23] X. Gou,[49] D. Grosnick,[60] W. Guryn,[6] A. I. Hamad,[29] A. Hamed,[5] S. Harabasz,[15] J. W. Harris,[64] S. He,[11] W. He,[18] X. H. He,[26] Y. He,[49] S. Heppelmann,[8] S. Heppelmann,[42] N. Herrmann,[19] E. Hoffman,[20] L. Holub,[14] Y. Hong,[31] S. Horvat,[64] Y. Hu,[18] H. Z. Huang,[9] S. L. Huang,[52] T. Huang,[37] X. Huang,[57] T. J. Humanic,[39] P. Huo,[52] G. Igo,[9,*] D. Isenhower,[1] W. W. Jacobs,[25] C. Jena,[23] A. Jentsch,[6] Y. Ji,[48] J. Jia,[6,52] K. Jiang,[48] S. Jowzaee,[63] X. Ju,[48] E. G. Judd,[7] S. Kabana,[53] M. L. Kabir,[10] S. Kagamaster,[32] D. Kalinkin,[25] K. Kang,[57] D. Kapukchyan,[10] K. Kauder,[6] H. W. Ke,[6] D. Keane,[29] A. Kechechyan,[28] M. Kelsey,[31] Y. V. Khyzhniak,[35] D. P. Kikoła,[62] C. Kim,[10] B. Kimelman,[8] D. Kincses,[16] T. A. Kinghorn,[8] I. Kisel,[17] A. Kiselev,[6] M. Kocan,[14] L. Kochenda,[35] L. K. Kosarzewski,[14] L. Kramarik,[14] P. Kravtsov,[35] K. Krueger,[4] N. Kulathunga Mudiyanselage,[20] L. Kumar,[41] S. Kumar,[26] R. Kunnawalkam Elayavalli,[63] J. H. Kwasizur,[25] R. Lacey,[52] S. Lan,[11] J. M. Landgraf,[6] J. Lauret,[6] A. Lebedev,[6] R. Lednicky,[28] J. H. Lee,[6] Y. H. Leung,[31] C. Li,[49] C. Li,[48] W. Li,[45] W. Li,[50] X. Li,[48] Y. Li,[57] Y. Liang,[29] R. Licenik,[38] T. Lin,[55] Y. Lin,[11] M. A. Lisa,[39] F. Liu,[11] H. Liu,[25] P. Liu,[52] P. Liu,[50] T. Liu,[64] X. Liu,[39] Y. Liu,[55] Z. Liu,[48] T. Ljubicic,[6] W. J. Llope,[63] R. S. Longacre,[6] N. S. Lukow,[54] S. Luo,[12] X. Luo,[11] G. L. Ma,[50] L. Ma,[18] R. Ma,[6] Y. G. Ma,[50] N. Magdy,[12] R. Majka,[64,*] D. Mallick,[36] S. Margetis,[29] C. Markert,[56] H. S. Matis,[31] J. A. Mazer,[46] N. G. Minaev,[43] S. Mioduszewski,[55] B. Mohanty,[36] I. Mooney,[63] Z. Moravcova,[14] D. A. Morozov,[43] M. Nagy,[16] J. D. Nam,[54] Md. Nasim,[22] K. Nayak,[11] D. Neff,[9] J. M. Nelson,[7] D. B. Nemes,[64] M. Nie,[49] G. Nigmatkulov,[35] T. Niida,[58] L. V. Nogach,[43] T. Nonaka,[58] A. S. Nunes,[6] G. Odyniec,[31] A. Ogawa,[6] S. Oh,[31] V. A. Okorokov,[35] B. S. Page,[6] R. Pak,[6] A. Pandav,[36] Y. Panebratsev,[28] B. Pawlik,[40] D. Pawlowska,[62] H. Pei,[11] C. Perkins,[7] L. Pinsky,[20] R. L. Pintér,[16] J. Pluta,[62] B. R. Pokhrel,[54] J. Porter,[31] M. Posik,[54] N. K. Pruthi,[41] M. Przybycien,[2] J. Putschke,[63] H. Qiu,[26] A. Quintero,[54] S. K. Radhakrishnan,[29] S. Ramachandran,[30] R. L. Ray,[56] R. Reed,[32] H. G. Ritter,[31] O. V. Rogachevskiy,[28] J. L. Romero,[8] L. Ruan,[6] J. Rusnak,[38] N. R. Sahoo,[49] H. Sako,[58] S. Salur,[46] J. Sandweiss,[64,*] S. Sato,[58] W. B. Schmidke,[6] N. Schmitz,[33] B. R. Schweid,[52] F. Seck,[15] J. Seger,[13] M. Sergeeva,[9] R. Seto,[10] P. Seyboth,[33] N. Shah,[24] E. Shahaliev,[28] P. V. Shanmuganathan,[6] M. Shao,[48] A. I. Sheikh,[29] W. Q. Shen,[50] S. S. Shi,[11] Y. Shi,[49] Q. Y. Shou,[50] E. P. Sichtermann,[31] R. Sikora,[2] M. Simko,[38] J. Singh,[41] S. Singha,[26] N. Smirnov,[64] W. Solyst,[25] P. Sorensen,[6] H. M. Spinka,[4,*] B. Srivastava,[44] T. D. S. Stanislaus,[60] M. Stefaniak,[62] D. J. Stewart,[64] M. Strikhanov,[35] B. Stringfellow,[44] A. A. P. Suaide,[47] M. Sumbera,[38] B. Summa,[42] X. M. Sun,[11] X. Sun,[12] Y. Sun,[48] Y. Sun,[21] B. Surrow,[54] D. N. Svirida,[3] P. Szymanski,[62] A. H. Tang,[6] Z. Tang,[48] A. Taranenko,[35] T. Tarnowsky,[34] J. H. Thomas,[31] A. R. Timmins,[20] D. Tlusty,[13] M. Tokarev,[28] C. A. Tomkiel,[32] S. Trentalange,[9] R. E. Tribble,[55] P. Tribedy,[6] S. K. Tripathy,[16] O. D. Tsai,[9] Z. Tu,[6] T. Ullrich,[6] D. G. Underwood,[4] I. Upsal,[49,6] G. Van Buren,[6] J. Vanek,[38] A. N. Vasiliev,[43] I. Vassiliev,[17] F. Videbæk,[6] S. Vokal,[28] S. A. Voloshin,[63] F. Wang,[44] G. Wang,[9] J. S. Wang,[21] P. Wang,[48] Y. Wang,[11] Y. Wang,[57] Z. Wang,[49] J. C. Webb,[6] P. C. Weidenkaff,[19] L. Wen,[9] G. D. Westfall,[34] H. Wieman,[31] S. W. Wissink,[25] R. Witt,[59] Y. Wu,[10] Z. G. Xiao,[57] G. Xie,[31] W. Xie,[44] H. Xu,[21] N. Xu,[31] Q. H. Xu,[49] Y. F. Xu,[50] Y. Xu,[49] Z. Xu,[6] Z. Xu,[9] C. Yang,[49] Q. Yang,[49] S. Yang,[6] Y. Yang,[37] Z. Yang,[11] Z. Ye,[45] Z. Ye,[12] L. Yi,[49] K. Yip,[6] Y. Yu,[49] H. Zbroszczyk,[62] W. Zha,[48] C. Zhang,[52] D. Zhang,[11] S. Zhang,[48] S. Zhang,[50] X. P. Zhang,[57] Y. Zhang,[48] Y. Zhang,[11] Z. J. Zhang,[37] Z. Zhang,[6] Z. Zhang,[12] J. Zhao,[44] C. Zhong,[50] C. Zhou,[50] X. Zhu,[57] Z. Zhu,[49] M. Zurek,[31] and M. Zyzak[17]

(STAR Collaboration)

[1]*Abilene Christian University, Abilene, Texas 79699*
[2]*AGH University of Science and Technology, FPACS, Cracow 30-059, Poland*

 © 2021 American Physical Society

[3]Alikhanov Institute for Theoretical and Experimental Physics NRC "Kurchatov Institute," Moscow 117218, Russia
[4]Argonne National Laboratory, Argonne, Illinois 60439
[5]American University of Cairo, New Cairo 11835, New Cairo, Egypt
[6]Brookhaven National Laboratory, Upton, New York 11973
[7]University of California, Berkeley, California 94720
[8]University of California, Davis, California 95616
[9]University of California, Los Angeles, California 90095
[10]University of California, Riverside, California 92521
[11]Central China Normal University, Wuhan, Hubei 430079
[12]University of Illinois at Chicago, Chicago, Illinois 60607
[13]Creighton University, Omaha, Nebraska 68178
[14]Czech Technical University in Prague, FNSPE, Prague 115 19, Czech Republic
[15]Technische Universität Darmstadt, Darmstadt 64289, Germany
[16]ELTE Eötvös Loránd University, Budapest, Hungary H-1117
[17]Frankfurt Institute for Advanced Studies FIAS, Frankfurt 60438, Germany
[18]Fudan University, Shanghai, 200433
[19]University of Heidelberg, Heidelberg 69120, Germany
[20]University of Houston, Houston, Texas 77204
[21]Huzhou University, Huzhou, Zhejiang 313000
[22]Indian Institute of Science Education and Research (IISER), Berhampur 760010, India
[23]Indian Institute of Science Education and Research (IISER) Tirupati, Tirupati 517507, India
[24]Indian Institute Technology, Patna, Bihar 801106, India
[25]Indiana University, Bloomington, Indiana 47408
[26]Institute of Modern Physics, Chinese Academy of Sciences, Lanzhou, Gansu 730000
[27]University of Jammu, Jammu 180001, India
[28]Joint Institute for Nuclear Research, Dubna 141 980, Russia
[29]Kent State University, Kent, Ohio 44242
[30]University of Kentucky, Lexington, Kentucky 40506-0055
[31]Lawrence Berkeley National Laboratory, Berkeley, California 94720
[32]Lehigh University, Bethlehem, Pennsylvania 18015
[33]Max-Planck-Institut für Physik, Munich 80805, Germany
[34]Michigan State University, East Lansing, Michigan 48824
[35]National Research Nuclear University MEPhI, Moscow 115409, Russia
[36]National Institute of Science Education and Research, HBNI, Jatni 752050, India
[37]National Cheng Kung University, Tainan 70101
[38]Nuclear Physics Institute of the CAS, Rez 250 68, Czech Republic
[39]The Ohio State University, Columbus, Ohio 43210
[40]Institute of Nuclear Physics PAN, Cracow 31-342, Poland
[41]Panjab University, Chandigarh 160014, India
[42]Pennsylvania State University, University Park, Pennsylvania 16802
[43]NRC "Kurchatov Institute," Institute of High Energy Physics, Protvino 142281, Russia
[44]Purdue University, West Lafayette, Indiana 47907
[45]Rice University, Houston, Texas 77251
[46]Rutgers University, Piscataway, New Jersey 08854
[47]Universidade de São Paulo, São Paulo, Brazil 05314-970
[48]University of Science and Technology of China, Hefei, Anhui 230026
[49]Shandong University, Qingdao, Shandong 266237
[50]Shanghai Institute of Applied Physics, Chinese Academy of Sciences, Shanghai 201800
[51]Southern Connecticut State University, New Haven, Connecticut 06515
[52]State University of New York, Stony Brook, New York 11794
[53]Instituto de Alta Investigación, Universidad de Tarapacá, Arica 1000000, Chile
[54]Temple University, Philadelphia, Pennsylvania 19122
[55]Texas A&M University, College Station, Texas 77843
[56]University of Texas, Austin, Texas 78712
[57]Tsinghua University, Beijing 100084
[58]University of Tsukuba, Tsukuba, Ibaraki 305-8571, Japan
[59]United States Naval Academy, Annapolis, Maryland 21402
[60]Valparaiso University, Valparaiso, Indiana 46383
[61]Variable Energy Cyclotron Centre, Kolkata 700064, India
[62]Warsaw University of Technology, Warsaw 00-661, Poland

[63]Wayne State University, Detroit, Michigan 48201
[64]Yale University, New Haven, Connecticut 06520

(Received 25 December 2020; accepted 1 April 2021; published 22 April 2021)

Global polarization of Ξ and Ω hyperons has been measured for the first time in Au + Au collisions at $\sqrt{s_{NN}} = 200$ GeV. The measurements of the Ξ^- and $\bar{\Xi}^+$ hyperon polarization have been performed by two independent methods, via analysis of the angular distribution of the daughter particles in the parity violating weak decay $\Xi \to \Lambda + \pi$, as well as by measuring the polarization of the daughter Λ hyperon, polarized via polarization transfer from its parent. The polarization, obtained by combining the results from the two methods and averaged over Ξ^- and $\bar{\Xi}^+$, is measured to be $\langle P_\Xi \rangle = 0.47 \pm 0.10(\text{stat}) \pm 0.23(\text{syst})\%$ for the collision centrality 20%–80%. The $\langle P_\Xi \rangle$ is found to be slightly larger than the inclusive Λ polarization and in reasonable agreement with a multiphase transport model. The $\langle P_\Xi \rangle$ is found to follow the centrality dependence of the vorticity predicted in the model, increasing toward more peripheral collisions. The global polarization of Ω, $\langle P_\Omega \rangle = 1.11 \pm 0.87(\text{stat}) \pm 1.97(\text{syst})\%$ was obtained by measuring the polarization of daughter Λ in the decay $\Omega \to \Lambda + K$, assuming the polarization transfer factor $C_{\Omega\Lambda} = 1$.

DOI: 10.1103/PhysRevLett.126.162301

The phenomenon of global polarization in heavy-ion collisions arises from the partial conversion of the orbital angular momentum of colliding nuclei into the spin angular momentum of the particles produced in the collision [1–3]. As a result, these particles become globally polarized along the direction of the initial orbital momentum of the nuclei. Global polarization was first observed by the STAR Collaboration in the beam energy scan Au + Au collisions [4] and was later confirmed, to better precision, in the analysis of the 200 GeV data with high statistics [5]. Assuming local thermal equilibrium, the polarization of the produced particles is determined by the local thermal vorticity of the fluid [3]. In the nonrelativistic limit (for hyperons $m_H \gg T$, where T is the temperature), the polarization of the particles is given by [6]

$$\mathbf{P} = \frac{\langle \mathbf{s} \rangle}{s} \approx \frac{(s+1)}{3} \frac{\boldsymbol{\omega}}{T}, \tag{1}$$

where s is the spin of the particle, $\langle \mathbf{s} \rangle$ is the mean spin vector, and $\boldsymbol{\omega} = \frac{1}{2} \boldsymbol{\nabla} \times \mathbf{v}$ is the local vorticity of the fluid velocity field. Averaged over the entire system volume, the vorticity direction should coincide with the direction of the system orbital momentum.

Following from Eq. (1), all particles, as well as anti-particles of the same spin, should have the same polarization. A difference could arise from effects of the initial magnetic field [6], from the fact that different particles are produced at different times or regions as the system freezes out [7], or through meson-baryon interactions [8]. Thus far, only Λ and $\bar{\Lambda}$ polarizations have been measured [4,5,9]. Therefore, to establish the global nature of the polarization, it is very important to measure the polarization of different particles, and if possible, particles of different spins. In the global polarization picture based on vorticity one expects different particles to be polarized in the same direction and that the polarization magnitudes for different particles depend only on their spin in accordance with Eq. (1).

In order to study the possible contribution from the initial magnetic field, the polarization measurement with particles of different magnetic moment would provide additional information. The difference in the polarization measured so far between Λ and $\bar{\Lambda}$ is not significant and is at the level of a couple standard deviations at most.

Although the energy dependence of the average Λ polarization can be explained well by theoretical models [7,10–14], many questions remain open, and the detail modeling of the global polarization and dynamical treatment of spin are under development. In fact, there exist sign problems in differential measurements of the global and local polarizations, not only between the experimental data and models but also among different models [15–17]. For example, Λ ($\bar{\Lambda}$) polarization along the beam direction measured experimentally [15] differ in the sign and magnitude of the effect from many theoretical calculations. Therefore, further experimental inputs are crucial for understanding the vorticity and polarization phenomena in heavy-ion collisions. In this paper we present the first measurements of the global polarization of spin $s = 1/2$ Ξ^- and $\bar{\Xi}^+$ hyperons, as well as spin $s = 3/2$ Ω hyperons in Au + Au collisions at $\sqrt{s_{\text{NN}}} = 200$ GeV.

Hyperon weak decays present the most straightforward possibility for measuring the polarization of the produced particles [18]. In parity-violating weak decays the daughter particle distribution in the rest frame of the hyperon directly depends on the hyperon polarization:

$$\frac{dN}{d\Omega^*} = \frac{1}{4\pi}(1 + \alpha_H \mathbf{P}_H^* \cdot \hat{\boldsymbol{p}}_B^*), \tag{2}$$

where α_H is the hyperon decay parameter, $\mathbf{P}_H^*$ is the hyperon polarization, and $\hat{\boldsymbol{p}}_B^*$ is the unit vector in the

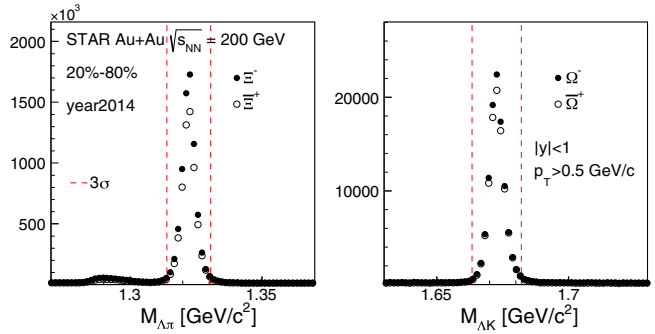

FIG. 1. Invariant mass distributions of Ξ^- ($\bar{\Xi}^+$) and Ω^- ($\bar{\Omega}^+$) for 20%–80% centrality in Au + Au collisions at $\sqrt{s_{NN}} = 200$ GeV taken in 2014. Vertical dashed lines indicate three standard deviations (3σ) from the peak positions, assuming a normal distribution.

direction of the daughter baryon momentum, both in the parent rest frame denoted by an asterisk.

Ξ^- ($\bar{\Xi}^+$) hyperon decay happens in two steps: $\Xi^- \to \Lambda + \pi^-$ with subsequent decay $\Lambda \to p + \pi^-$. If Ξ^- is polarized, its polarization is partially transferred to the daughter Λ. Both steps in such a cascade decay are parity violating and thus can be used for an independent measurement of the polarization of Ξ^- ($\bar{\Xi}^+$).

The polarization of the daughter baryon in a weak decay of a spin 1/2 hyperon is described by the Lee-Yang formula [19–21] in terms of the three parameters α (parity violating part), β (violation of the time reversal symmetry), and γ (satisfying $\alpha^2 + \beta^2 + \gamma^2 = 1$). For a particular case of $\Xi \to \Lambda + \pi$ decay it reads:

$$\mathbf{P}^*_\Lambda = \frac{(\alpha_\Xi + \mathbf{P}^*_\Xi \cdot \hat{\boldsymbol{p}}^*_\Lambda)\hat{\boldsymbol{p}}^*_\Lambda + \beta_\Xi \mathbf{P}^*_\Xi \times \hat{\boldsymbol{p}}^*_\Lambda + \gamma_\Xi \hat{\boldsymbol{p}}^*_\Lambda \times (\mathbf{P}^*_\Xi \times \hat{\boldsymbol{p}}^*_\Lambda)}{1 + \alpha_\Xi \mathbf{P}^*_\Xi \cdot \hat{\boldsymbol{p}}^*_\Lambda}, \tag{3}$$

where $\hat{\boldsymbol{p}}^*_\Lambda$ is the unit vector of the Λ momentum in the Ξ rest frame. Averaging over the angular distribution of the Λ in the rest frame of the Ξ given by Eq. (2) yields

$$\mathbf{P}^*_\Lambda = C_{\Xi^-\Lambda}\mathbf{P}^*_\Xi = \frac{1}{3}(1 + 2\gamma_\Xi)\mathbf{P}^*_\Xi. \tag{4}$$

Using the measured value for the γ_Ξ parameter [21,22], the polarization transfer coefficient for Ξ^- to Λ decay is

$$C_{\Xi^-\Lambda} = \frac{1}{3}(1 + 2 \times 0.916) = +0.944. \tag{5}$$

The polarization of the daughter baryon in a two particle decay of spin 3/2 hyperon, $\Omega \to \Lambda + K$, is also described by three parameters α_Ω, β_Ω, and γ_Ω [23]. The decay parameter α_Ω determines the angular distribution of Λ in the Ω rest frame and is measured to be small [22]: $\alpha_\Omega = 0.0157 \pm 0.0021$; this makes it practically impossible to measure the Ω polarization via analysis of the daughter Λ angular distribution. The polarization transfer in this case is determined by the γ_Ω parameter via [23–25]

$$\mathbf{P}^*_\Lambda = C_{\Omega^-\Lambda}\mathbf{P}^*_\Omega = \frac{1}{5}(1 + 4\gamma_\Omega)\mathbf{P}^*_\Omega. \tag{6}$$

The time-reversal violation parameter β_Ω is expected to be small. This combined with the constraint that $\alpha^2 + \beta^2 + \gamma^2 = 1$ limits the unmeasured parameter to $\gamma_\Omega \approx \pm 1$, resulting in a polarization transfer $C_{\Omega^-\Lambda} \approx 1$ or $C_{\Omega^-\Lambda} \approx -0.6$.

Our analysis is based on the data of Au + Au collisions at $\sqrt{s_{NN}} = 200$ GeV collected in 2010, 2011, 2014, and 2016 by the STAR detector. Charged-particle tracks were measured in the time projection chamber (TPC) [26], which covers the full azimuth and a pseudorapidity range of $|\eta| < 1$. The collision vertices were reconstructed using the measured charged-particle tracks and were required to be within 30 cm relative to the TPC center in the beam direction for the 2010 and 2011 datasets to ensure a good acceptance of reconstructed tracks. The narrower vertex selection to be within 6 cm was applied in the 2014 and 2016 data due to an online trigger requirement for the heavy flavor tracker installed prior to 2014 data taking. The vertex in the radial direction relative to the beam center was also required to be within 2 cm to reject background from collisions with a beam pipe. Additionally, the difference in the vertex positions along the beam direction from the vertex position detectors (VPD) [27] located at forward and backward pseudorapidities ($4.24 < |\eta| < 5.1$) was required to be less than 3 cm to suppress pileup events in which more than one heavy-ion collision occurred. These selection criteria yielded about 180×10^6 (350×10^6) minimum bias (MB) events for the 2010 (2011) dataset, 1×10^9 MB events for the 2014 dataset, and 1.5×10^9 MB events for the 2016 dataset. The MB trigger requires hits of both VPDs and the zero-degree calorimeters (ZDCs) [28], which detect spectator neutrons in $|\eta| > 6.3$. The collision centrality was determined from the measured multiplicity of charged particles within $|\eta| < 0.5$ and a Monte Carlo Glauber simulation [29,30].

The first-harmonic event plane angle Ψ_1 as an experimental estimate of the impact parameter direction was determined by measuring the neutron spectator deflection [31] in the ZDCs equipped with shower maximum detectors [32–34]. The event plane resolution [35] is largest (~41%; the resolution is better if it is closer to 100%) at 30%–40% collision centrality for the 2014 and 2016 datasets, and is decreased by 4% for the 2010 and 2011 datasets [5].

The parent Ξ^- ($\bar{\Xi}^+$), Ω^- ($\bar{\Omega}^+$), and their daughter Λ ($\bar{\Lambda}$) were reconstructed utilizing the decay channels of $\Xi^- \to \Lambda\pi^-$ (99.887%), $\Omega^- \to \Lambda K^-$ (67.8%), and $\Lambda \to p\pi^-$ (63.9%), where the numbers in parentheses indicate the corresponding branching ratio of the decays [22]. Charged

pions (kaons) and protons of the daughter particles were identified based on the ionization energy loss in the TPC gas, and the timing information measured by the time-of-flight detector [36]. Reconstruction of Ξ^- ($\bar{\Xi}^+$), Ω^- ($\bar{\Omega}^+$), and Λ ($\bar{\Lambda}$) was performed using the KF particle finder package based on the Kalman filter (KF) method initially developed for the CBM and ALICE experiments [37–39], which utilizes the quality of the track fit as well as the decay topology. Figure 1 shows the invariant mass distributions for reconstructed Ξ^- ($\bar{\Xi}^+$) and Ω^- ($\bar{\Omega}^+$) for 20%–80% centrality. The purities for this centrality bin are higher than 90% for both species. The significance with the Kalman filter method is found to be increased by ~30% for Ξ compared to the traditional method for reconstruction of short-lived particles (e.g. see Refs. [5,40]). The hyperon candidates were also ensured not to share their decay products with other particles of interest.

The polarization along the initial angular momentum direction can be defined as [41]

$$P_H = \frac{8}{\pi \alpha_H} \frac{\langle \sin(\Psi_1^{\rm obs} - \phi_B^*) \rangle}{\mathrm{Res}(\Psi_1)}, \tag{7}$$

where α_H is the hyperon decay parameter and ϕ_B^* is the azimuthal angle of the daughter baryon in the parent hyperon rest frame. The azimuthal angle of the first-order event plane is $\Psi_1^{\rm obs}$, and $\mathrm{Res}(\Psi_1)$ is the resolution [35] with which it estimates the reaction plane.

The extraction of $\langle \sin(\Psi_1^{\rm obs} - \phi^*) \rangle$ was performed in the same way as in our previous studies [4,5]. The decay parameters of Λ, Ξ^-, and Ω^- have been recently updated by the Particle Data Group [22] and the latest values are used in this analysis; $\alpha_\Lambda = 0.732 \pm 0.014$, $\alpha_\Xi = -0.401 \pm 0.010$, and $\alpha_\Omega = 0.0157 \pm 0.0021$. When comparing to earlier measurements, the previous results are rescaled by using the new values, i.e. $\alpha_{\rm old}/\alpha_{\rm new}$. In case of the Ξ and Ω hyperon polarization measurements via measurements of the daughter Λ polarization, the polarization transfer factors $C_{\Xi\Lambda(\Omega\Lambda)}$ from Eqs. (4) and (6) are used to obtain the parent polarization.

The largest systematic uncertainty (37%) was attributed to the variation of the results obtained with datasets taken in different years. The difference could be partly due to the change in the detector configuration (inclusion of the heavy flavor tracker in the 2014 and 2016 data taking) and increased luminosity in recent years, both of which lead to the reduction of detecting efficiency. After careful checks of the detector performance and detailed quality assurance of the data, weighted average over different datasets was used as the final result. All other systematic uncertainties were assessed based on the weighted average: by comparing different polarization signal extractions [5] (11%), by varying the mass window for particles of interest from 3σ to 2σ (15%), by varying the decay lengths of both parent and daughter hyperons (4%), and by considering uncertainties on the decay parameter α_H (2%), where the numbers in parentheses represent the uncertainty for the Ξ polarization via the daughter Λ polarization measurement. A correction for nonuniform acceptance effects [41] was applied for the appropriate detector configuration for the given dataset. This correction, depending on particle species, was less than 2%. Due to a weak p_T dependence on the global polarization [5], effects from the p_T dependent efficiency of the hyperon reconstruction were found to be negligible.

Figure 2 shows the collision energy dependence of the Λ hyperon global polarization measured earlier [4,5,9,41] together with the new results on Ξ and Ω global polarizations at $\sqrt{s_{NN}} = 200$ GeV. (Note that the statistical and systematic uncertainties for the Λ are smaller than the symbol size.) For both Ξ and Ω polarizations, the particle and antiparticle results are averaged to reduce the statistical uncertainty. Also to maximize the significance of the polarization signal, the results were integrated over the centrality range 20%–80%, transverse momentum $p_T > 0.5$ GeV/c, and rapidity $|y| < 1$. Global polarization of Ξ^- and $\bar{\Xi}^+$ measurements via daughter Λ polarization show positive values, with no significant difference between Ξ^- and $\bar{\Xi}^+$ [$P_\Xi(\%) = 0.77 \pm 0.16(\mathrm{stat}) \pm 0.49(\mathrm{syst})$ and $P_{\bar{\Xi}}(\%) = 0.49 \pm 0.16(\mathrm{stat}) \pm 0.20(\mathrm{syst})$]. The average polarization value obtained by this method is $\langle P_\Xi \rangle(\%) = 0.63 \pm 0.11(\mathrm{stat}) \pm 0.26(\mathrm{syst})$. The $\Xi + \bar{\Xi}$ polarization was

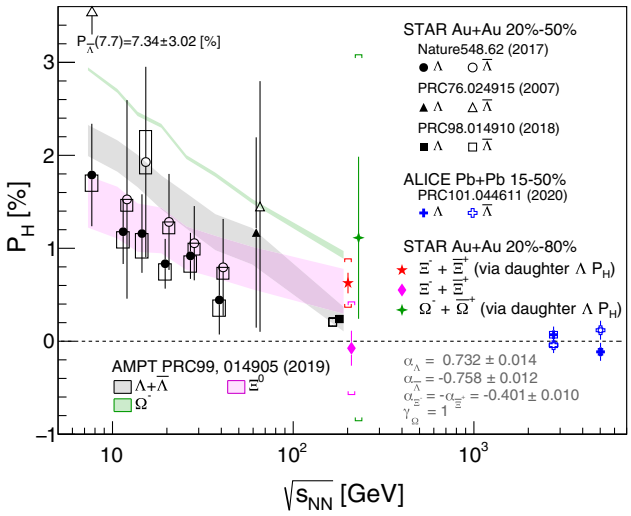

FIG. 2. The energy dependence of the hyperon global polarization measurements. The points corresponding to Λ and $\bar{\Lambda}$ polarizations, as well as Ξ and Ω points in Au + Au collisions at $\sqrt{s_{\rm NN}} = 200$ GeV are slightly shifted for clarity. Previous results from the STAR [4,5,41] and ALICE [9] experiments compared here are rescaled by new decay parameter indicated inside the figure. The data point for $\bar{\Lambda}$ at 7.7 GeV is out of the axis range and indicated by an arrow with the value. The results of the AMPT model calculations [42] for 20%–50% centrality are shown by shaded bands where the band width corresponds to the uncertainty of the calculations.

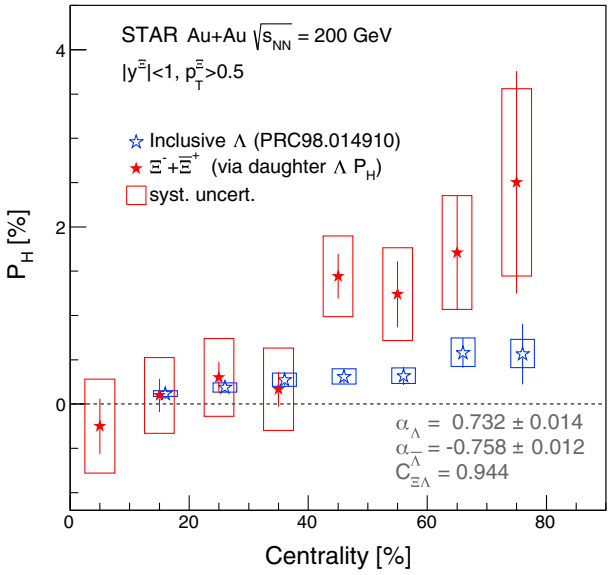

FIG. 3. The global polarization of Ξ hyperons obtained via measurements of the polarization of daughter Λ hyperons as a function of the collision centrality in Au + Au collisions at $\sqrt{s_{NN}} = 200$ GeV. Open boxes show the systematic uncertainties. Results for the inclusive Λ measurements [5] are shown for comparison.

also measured via analysis of the angular distribution of daughter Λ in Ξ rest frame. This result, $\langle P_\Xi \rangle(\%) = -0.07 \pm 0.19(\text{stat}) \pm 0.50(\text{syst})$, has larger uncertainty in part due to a smaller value of α_Ξ compared to α_Λ, which leads to smaller sensitivity of the measurement. Note that with given uncertainties the difference between the two methods is within 1 σ. The weighted average of the two measurements is $\langle P_\Xi \rangle(\%) = 0.47 \pm 0.10(\text{stat}) \pm 0.23(\text{syst})$, which is larger than the polarization of inclusive $\Lambda + \bar{\Lambda}$ measured at the same energy for 20%–80% centrality, $\langle P_\Lambda \rangle(\%) = 0.24 \pm 0.03 \pm 0.03$ [5], although the difference is still not significant considering the statistical and systematic uncertainties of both measurements. Note that the above quoted values for the inclusive Λ have been rescaled by the new decay parameter as mentioned earlier and "inclusive" means Λ coming from a primary vertex as well as those decaying from higher states.

Calculations [42] carried out with a multiphase transport model (AMPT) can describe the particle species dependence in data at 200 GeV as well as the energy dependence for Λ. These calculations indicate that the lighter particles with higher spin could be more polarized by the vorticity [42]. The multistrange particles might freeze out at earlier times, which may lead to larger polarization for Ξ and Ω compared to Λ [7]. The feed-down effect can also lead to a 15%–20% reduction of the primary Λ polarization [6,10,11,43], while the Ξ has less contribution from the feed-down. All these effects can contribute to small differences in the measured polarizations between inclusive Λ and Ξ hyperons.

Global polarization of Ω^- was also measured and is presented in Fig. 2 under the assumption of $\gamma_\Omega = +1$ and therefore $C_{\Omega\Lambda} = 1$, as discussed with respect to Eq. (6). The result has large uncertainty, $\langle P_\Omega \rangle(\%) = 1.11 \pm 0.87(\text{stat}) \pm 1.97(\text{syst})$ for 20%–80% centrality. Assumption of $\gamma_\Omega = -1$ (therefore $C_{\Omega\Lambda} = -0.6$) results in $\langle P_\Omega \rangle(\%) = -0.67 \pm 0.52(\text{stat}) \pm 1.18(\text{syst})$. Assuming the validity of the global polarization picture, $\langle P_\Omega \rangle$ should be positive, and therefore the result favors $\gamma_\Omega \approx +1$ instead of $\gamma_\Omega \approx -1$, but the uncertainties are large and more precise measurements are needed to make a definitive statement.

The centrality dependence of $\Xi + \bar{\Xi}$ polarization via the measurement of daughter Λ polarization is shown in Fig. 3, where the inclusive Λ polarization [5] is plotted for comparison. The hyperon polarization increases in more peripheral collisions as expected from the centrality dependence of the fluid vorticity [13,44]. The Ξ polarization looks larger than that of the inclusive Λ in peripheral collisions as already discussed in relation to Fig. 2, although the uncertainties preclude a more definite conclusion.

In summary, we have presented the first measurements of the global polarization for Ξ^- ($\bar{\Xi}^+$) hyperons in Au + Au collisions at $\sqrt{s_{NN}} = 200$ GeV. Our results of Ξ hyperon polarization, along with the previous measurements of Λ polarization, confirm the global polarization picture based on the system fluid vorticity. The average polarization of $\Xi + \bar{\Xi}$ seems to be larger than that of the inclusive Λ, which is qualitatively captured by the AMPT model. The measured polarization seems to exhibit a centrality dependence as expected from the impact parameter dependence of the vorticity. Global polarization of Ω^- hyperons was, also for the first time, extracted via measurements of the polarization of the daughter Λ and presented with the assumption that $\gamma_\Omega = +1$. Future measurements with higher precision will shed light on the uncertainty of the decay parameter γ_Ω, as well as experimental results on the global polarization of spin-3/2 particles, providing critical information about spin dynamics in heavy-ion collisions.

We thank the RHIC Operations Group and RCF at BNL, the NERSC Center at LBNL, and the Open Science Grid consortium for providing resources and support. This work was supported in part by the Office of Nuclear Physics within the U.S. DOE Office of Science, the U.S. National Science Foundation, the Ministry of Education and Science of the Russian Federation, National Natural Science Foundation of China, Chinese Academy of Science, the Ministry of Science and Technology of China and the Chinese Ministry of Education, the Higher Education Sprout Project by Ministry of Education at NCKU, the National Research Foundation of Korea, Czech Science Foundation and Ministry of Education, Youth and Sports of the Czech Republic, Hungarian National Research, Development and Innovation Office, New National

Excellency Programme of the Hungarian Ministry of Human Capacities, Department of Atomic Energy and Department of Science and Technology of the Government of India, the National Science Centre of Poland, the Ministry of Science, Education and Sports of the Republic of Croatia, RosAtom of Russia and German Bundesministerium für Bildung, Wissenschaft, Forschung and Technologie (BMBF), Helmholtz Association, Ministry of Education, Culture, Sports, Science, and Technology (MEXT) and Japan Society for the Promotion of Science (JSPS).

[*]Deceased.

[1] Z.-T. Liang and X.-N. Wang, Globally Polarized Quark-Gluon Plasma in Noncentral A + A Collisions, Phys. Rev. Lett. **94**, 102301 (2005); Phys. Rev. Lett. **96**, 039901(E) (2006).

[2] S. A. Voloshin, Polarized secondary particles in unpolarized high energy hadron-hadron collisions?, arXiv:nucl-th/0410089.

[3] F. Becattini, F. Piccinini, and J. Rizzo, Angular momentum conservation in heavy ion collisions at very high energy, Phys. Rev. C **77**, 024906 (2008).

[4] L. Adamczyk *et al.* (STAR Collaboration), Global Λ hyperon polarization in nuclear collisions, Nature (London) **548**, 62 (2017).

[5] J. Adam *et al.* (STAR Collaboration), Global polarization of Λ hyperons in Au Au + Au collisions at $\sqrt{s_{NN}} = 200$ GeV, Phys. Rev. C **98**, 014910 (2018).

[6] F. Becattini, I. Karpenko, M. A. Lisa, I. Upsal, and S. Voloshin, Global hyperon polarization at local thermodynamic equilibrium with vorticity, magnetic field and feed-down, Phys. Rev. C **95**, 054902 (2017).

[7] O. Vitiuk, L. V. Bravina, and E. E. Zabrodin, Is different Λ and $\bar{\Lambda}$ polarization caused by different spatio-temporal freeze-out picture?, Phys. Lett. B **803**, 135298 (2020).

[8] L. P. Csernai, J. I. Kapusta, and T. Welle, Λ and $\bar{\Lambda}$ spin interaction with meson fields generated by the baryon current in high energy nuclear collisions, Phys. Rev. C **99**, 021901(R) (2019).

[9] S. Acharya *et al.* (ALICE Collaboration), Global polarization of $\Lambda\bar{\Lambda}$ hyperons in Pb-Pb collisions at $\sqrt{s_{NN}} = 2.76$ and 5.02 TeV, Phys. Rev. C **101**, 044611 (2020).

[10] I. Karpenko and F. Becattini, Study of Λ polarization in relativistic nuclear collisions at $\sqrt{s_{NN}} = 7.7$–200 GeV, Eur. Phys. J. C **77**, 213 (2017).

[11] H. Li, L. G. Pang, Q. Wang, and X. L. Xia, Global Λ polarization in heavy-ion collisions from a transport model, Phys. Rev. C **96**, 054908 (2017).

[12] Y. Sun and C. M. Ko, Λ hyperon polarization in relativistic heavy ion collisions from a chiral kinetic approach, Phys. Rev. C **96**, 024906 (2017).

[13] Y. Xie, D. Wang, and L. P. Csernai, Global Λ polarization in high energy collisions, Phys. Rev. C **95**, 031901(R) (2017).

[14] Y. B. Ivanov, V. D. Toneev, and A. A. Soldatov, Estimates of hyperon polarization in heavy-ion collisions at collision energies $\sqrt{s_{NN}} = 4$–40 GeV, Phys. Rev. C **100**, 014908 (2019).

[15] Jaroslav Adam *et al.* (STAR Collaboration), Polarization of Λ ($\bar{\Lambda}$) Hyperons along the Beam Direction in Au + Au Collisions at $\sqrt{s_{NN}} = 200$ GeV, Phys. Rev. Lett. **123**, 132301 (2019).

[16] T. Niida (STAR Collaboration), Global and local polarization of Λ hyperons in Au + Au collisions at 200 GeV from STAR, Nucl. Phys. **A982**, 511 (2019).

[17] F. Becattini and M. A. Lisa, Polarization and vorticity in the quark gluon plasma, Annu. Rev. Nucl. Part. Sci. **70**, 395 (2020).

[18] G. Bunce *et al.*, Λ^0 Hyperon Polarization in Inclusive Production by 300-GeV Protons on Beryllium, Phys. Rev. Lett. **36**, 1113 (1976).

[19] T. D. Lee and C.-N. Yang, General partial wave analysis of the decay of a hyperon of spin 1/2, Phys. Rev. **108**, 1645 (1957).

[20] K. B. Luk *et al.* (E756 Collaboration), Search for Direct *CP* Violation in Nonleptonic Decays of Charged Ξ and Λ Hyperons, Phys. Rev. Lett. **85**, 4860 (2000).

[21] M. Huang, R. A. Burnstein, A. Chakravorty, Y. C. Chen, W. S. Choong *et al.* (HyperCP Collaboration), New Measurement of $\Xi \to \Lambda\pi^-$ Decay Parameters, Phys. Rev. Lett. **93**, 011802 (2004).

[22] P. A. Zyla *et al.* (Particle Data Group), Review of particle physics, Prog. Theor. Exp. Phys. **2020**, 083C01 (2020).

[23] K. B. Luk, A. Beretvas, L. Deck, T. Devlin, R. Rameika *et al.*, New measurements of properties of the Ω^- hyperon, Phys. Rev. D **38**, 19 (1988).

[24] K.-B. Luk, A study of the omega-hyperon, Ph.D. thesis, Rutgers University, Piscataway, NJ, 1983.

[25] J. Kim, J. Lee, J. S. Shim, and H. S. Song, Polarization effects in spin 3/2 hyperon decay, Phys. Rev. D **46**, 1060 (1992).

[26] M. Anderson *et al.*, The STAR time projection chamber: A unique tool for studying high multiplicity events at RHIC, Nucl. Instrum. Methods Phys. Res., Sect. A **499**, 659 (2003).

[27] W. J. Llope *et al.*, The STAR vertex position detector, Nucl. Instrum. Methods Phys. Res., Sect. A **759**, 23 (2014).

[28] C. Adler, A. Denisov, E. Garcia, M. Murray, H. Strobele, and S. White, The RHIC zero degree calorimeters, Nucl. Instrum. Methods Phys. Res., Sect. A **461**, 337 (2001).

[29] M. L. Miller, K. Reygers, S. J. Sanders, and P. Steinberg, Glauber modeling in high-energy nuclear collisions, Annu. Rev. Nucl. Part. Sci. **57**, 205 (2007).

[30] L. Adamczyk *et al.* (STAR Collaboration), Inclusive charged hadron elliptic flow in Au + Au collisions at $\sqrt{s_{NN}} = 7.7$–39 GeV, Phys. Rev. C **86**, 054908 (2012).

[31] S. A. Voloshin and T. Niida, Ultra-relativistic nuclear collisions: Direction of spectator flow, Phys. Rev. C **94**, 021901(R) (2016).

[32] STAR Note, SN0448: Proposed addition of a shower max detector to the STAR zero degree calorimeters, https://drupal.star.bnl.gov/STAR/starnotes/public/sn0448.

[33] J. Adams *et al.* (STAR Collaboration), Directed flow in Au + Au collisions at $\sqrt{s_{NN}} = 62.4$ GeV, Phys. Rev. C **73**, 034903 (2006).

[34] L. Adamczyk *et al.* (STAR Collaboration), Azimuthal anisotropy in Cu + Au collisions at $\sqrt{s_{NN}} = 200$ GeV, Phys. Rev. C **98**, 014915 (2018).

[35] A. M. Poskanzer and S. A. Voloshin, Methods for analyzing anisotropic flow in relativistic nuclear collisions, Phys. Rev. C **58**, 1671 (1998).

[36] W. J. Llope, Multigap RPCs in the STAR experiment at RHIC, Nucl. Instrum. Methods Phys. Res., Sect. A **661**, S110 (2012).

[37] S. Gorbunov, On-line reconstruction algorithms for the CBM and ALICE experiments, Ph.D. thesis, Johann Wolfgang Goethe-Universität, 2013.

[38] M. Zyzak, Online selection of short-lived particles on many-core computer architectures in the CBM experiment at FAIR, Ph.D. thesis, Johann Wolfgang Goethe-Universität, 2016.

[39] I. Kisel (CBM Collaboration), Event topology reconstruction in the CBM experiment, J. Phys. Conf. Ser. **1070**, 012015 (2018).

[40] J. Adam *et al.* (STAR Collaboration), Strange hadron production in $\mathrm{Au}+\mathrm{Au}$ collisions at $\sqrt{s_{NN}}=7.7$, 11.5, 19.6, 27, and 39 GeV, Phys. Rev. C **102**, 034909 (2020).

[41] B. I. Abelev *et al.* (STAR Collaboration), Global polarization measurement in $\mathrm{Au}+\mathrm{Au}$ collisions, Phys. Rev. C **76**, 024915 (2007); Phys. Rev. C **95**, 039906(E) (2017).

[42] D.-X. Wei, W.-T. Deng, and X.-G. Huang, Thermal vorticity and spin polarization in heavy-ion collisions, Phys. Rev. C **99**, 014905 (2019).

[43] X.-L. Xia, H. Li, X.-G. Huang, and H. Z. Huang, Feed-down effect on Λ spin polarization, Phys. Rev. C **100**, 014913 (2019).

[44] Y. Jiang, Z.-W. Lin, and J. Liao, Rotating quark-gluon plasma in relativistic heavy ion collisions, Phys. Rev. C **94**, 044910 (2016); Phys. Rev. C **95**, 049904(E) (2017).